Bistability of the Sn Donor in $Al_xGa_{1-x}As$ and GaAs under Pressure Evidenced by Mössbauer Spectroscopy

D.L. Williamson [1]
P. Gibart [2]

Deep donor levels have been observed in $Al_xGa_{1-x}As$ for $x > 0.22$ and GaAs under hydrostatic pressure (for $p > 2GPa$). Persistent photoconduction (PPC) is the most striking feature of this deep donor, the DX center. Upon illumination at low temperature, the free electron concentration increases and remains at this new value even after the light is off. Basically the DX centers are photoionized and one (or several) electrons per center are transferred to the conduction band. The bistable character of donor, which involves two electronic configurations, can be studied by Mössbauer spectroscopy (MS).

MS is one of the few techniques that can provide atomic-scale information on doping-related defects in semiconductors. Electronic wavefunctions, near-neighbor geometries and lattice vibrational properties can be probed. Mössbauer spectroscopy has recently been used to observe the Sn DX center in $Al_xGa_{1-x}As$ near $x = 0.3 - 0.4$ and in GaAs under high pressure. The latter experiment, coupled with Hall data, provides strong evidence that the Sn DX center localizes two or more electrons in the ground state. The existence of a large lattice relaxation at the DX site, detectable through the electric quadrupole interaction, has not yet been established.

I. Introduction

The ternary semiconductor alloy system $Al_xGa_{1-x}As$ has been and is being extensively studied because of its importance and further promise in high-speed and optoelectronic devices. Its value stems primarily from the ability to adjust the band gap (via suitable x) without changing the lattice constant, a crucial consideration in epitaxial growth. However, a severe problem arises in association with n-type doping of $Al_xGa_{1-x}As$. Independent of the nature of the dopant and the epitaxial-growth method, donor incorporation leads to similar features : for $x < 0.2$ the dopant introduces a shallow level a few meV from the conduction band ; for $x > 0.2$, in addition to the shallow donor, a deep donor appears with a thermal activation of the order of 10^2 meV ; furthermore, in this compositional range persistent photoconductivity (PPC) is observed [1]. The deep level, the so-called "DX center", is a substitutional donor that is most often associated with the L-band minimum [2-10]. Several recent studies have shown that in the region of interest, $0.2 < x < 0.7$, shallow and deep donors exist simultaneously [8-10].

I.1. Electrical and Optical Properties of the DX Center in $Al_xGa_{1-x}As$

In $Al_xGa_{1-x}As$, the DX is the lowest energy state of the substitutional donor for $x > 0.22$. For $x < 0.22$, DX exists as a resonant state in the Γ continuum *(figure 1)*. The observation of DX-like behaviour in different semiconductor alloys ($Al_xGa_{1-x}As$, $GaAs_xP_{1-x}$...) leads to the straightforward conclusion that DX is related to the particular band structure of these alloys where the Γ, L, and X valleys are close together. As hydrostatic pressure applied to GaAs changes the band structure, similar to the effect of Al alloying (one percent increase in Al is approximately equivalent to 0.1 GPa increase in pressure), DX appears in the band gap for $p > 2GPa$ *(figure 2)*. The striking features about DX centers are the large binding energy, and the capture (and emission) barrier which controls the transition rate of electrons from (and

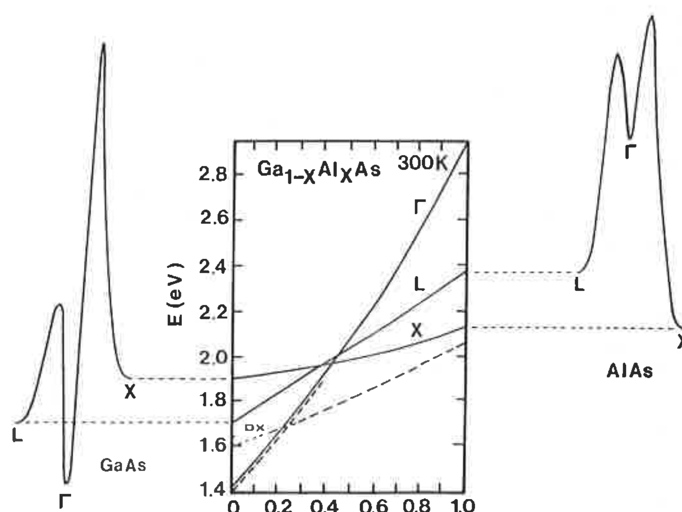

FIGURE 1. - *Variation of the Γ, L and X minima in the $Al_xGa_{1-x}As$ alloys as a function of x. On the GaAs and AlAs side, conduction bands for x = 0 and x = 1 respectively.*

1 Department of Physics, Colorado School of Mines, Golden, Colorado 80401, USA.
2 Laboratoire de physique du solide et énergie solaire, CNRS, Sophia Antipolis, 06560 Valbonne, France.

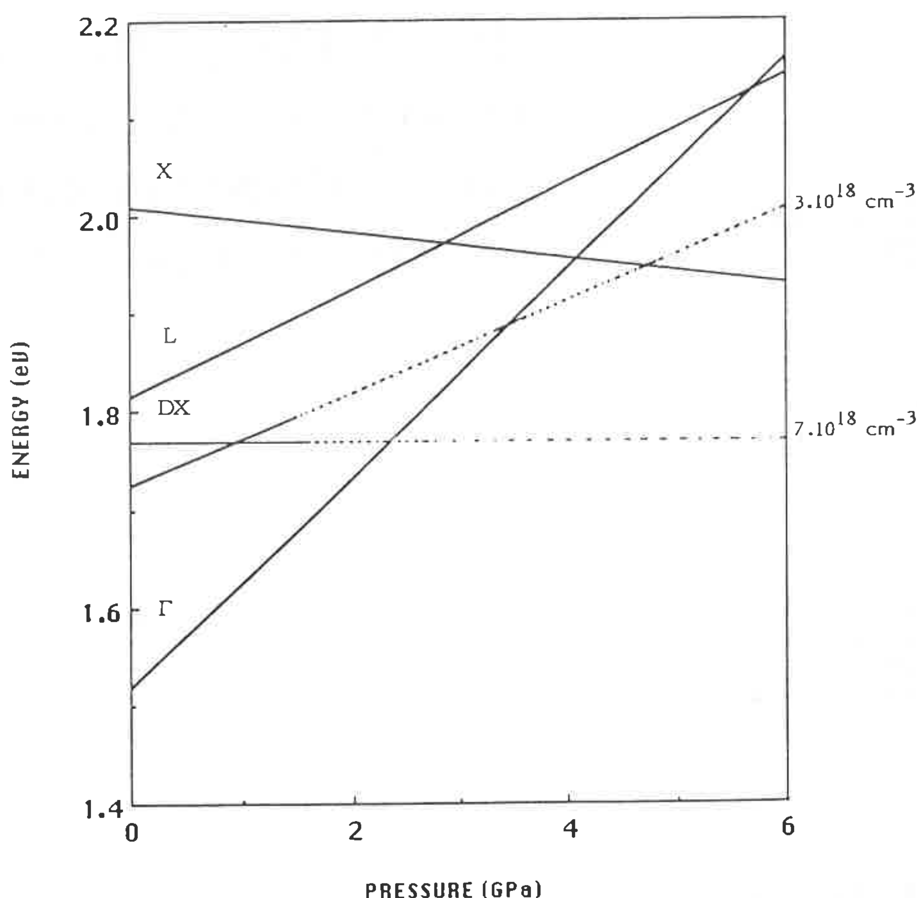

FIGURE 2. - *Variation of the direct and indirect band gaps in GaAs as a function of hydrostatic pressure.*

to) the DX center. At low temperatures, 20-135 K depending of the nature of the n impurity, capture and emission of electrons are impossible.

When plotting the Hall carrier concentration as a function of 1/T (for x > 0.22) a double slope behaviour appears. In addition, an apparent deepening of the donor level with x is noted for any n-type dopant. At thermal equilibrium, the free electron concentration is determined by the donor binding energy E_d. For a non-degenerate semiconductor :

$$n \approx (N_D - N_A / 2N_A)\, N_C \exp(-E_d / kT)$$

where, n, N_D, N_A have their usual meaning and N_C is the effective density of states in the conduction band. Accounting for the distribution of electrons in the different Γ, L and X valleys, the total carrier density will be :

$$n = n_\Gamma + n_L + n_X \qquad (1)$$

When the temperature is lowered below about 20-135 K, electron capture to the DX state is no longer possible, and carriers remain in the Γ valley. Then, when shallow donors are present, the freeze out would occur to this shallow level. Therefore, below 100 K, one can write

$$(n_\Gamma)_{4K} = (n_\Gamma + n_L + n_X)_{100K} \qquad (2)$$

From the neutrality equation

$$n_\Gamma + n_L + n_X = N_D - \frac{N_D}{1 + 1/g \exp(E_D - E_F/kT)} \qquad (3)$$

the activation energy E_d of the DX level can be determined.

In $Al_xGa_{1-x}As$, the very same substitutional donor can exist as a deep donor, the DX center, and also as a hydrogenelike shallow donor linked to the Γ band. The electronic and optical properties of $Al_xGa_{1-x}As$ arise from the bistability of this substitutional donor.

Upon illumination at low temperatures the free electron concentration in n-$Al_xGa_{1-x}As$ (with x > 0.22) increases to about the room temperature value and remains at this new value when the light is off. This is the persistent photoconductivity (PPC) which disappears at T > 100 K *(figure 3)*. This PPC is due to the capture barrier in the configuration coordinate (CC) diagram and is directly related to the microscopic nature of the DX center.

For describing the properties of deep centers, a configuration coordinate diagram (CC) is a useful tool. It gives the sum of elastic and electronic energy for different charge states of a defect when a change in lattice configuration is involved. A CC diagram consists of several parabolas placed at proper energy positions as a function of a generalized lattice coordinate Q *(figure 4)*. The parabolas shown on the left represents the total energy when an electron lies in the conduction band (DX ionized) whereas the parabola on the right corresponds to occupied DX level. The shift in Q indicates the change in microscopic configuration of the donor when the charge state of the DX level changes. One of the current controversies about DX centers is whether the lattice relaxation associated with the defect is large (LLR) or small (SLR) [1].

I.2. Mössbauer Spectroscopy in Semiconductors : Introduction

The Mössbauer effect is a probe of the atomic-scale nature of solids that has seen many applications in the study of semiconductors [11-13]. Through the interactions of nucleons and atomic electrons, this nuclear spectroscopic method provides specific

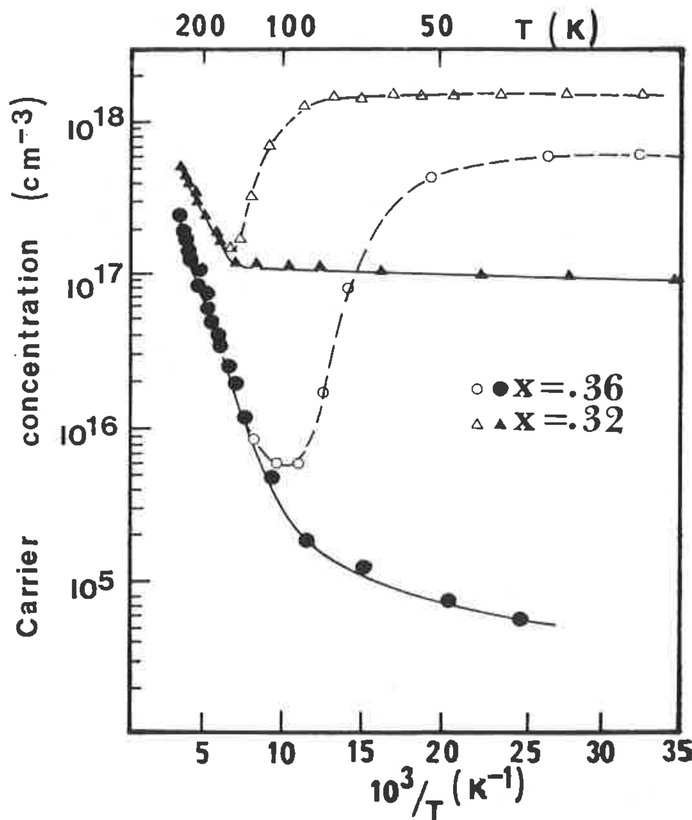

FIGURE 3. - *Hall concentration of n-doped $Al_xGa_{1-x}As$ in the dark and under illumination.*

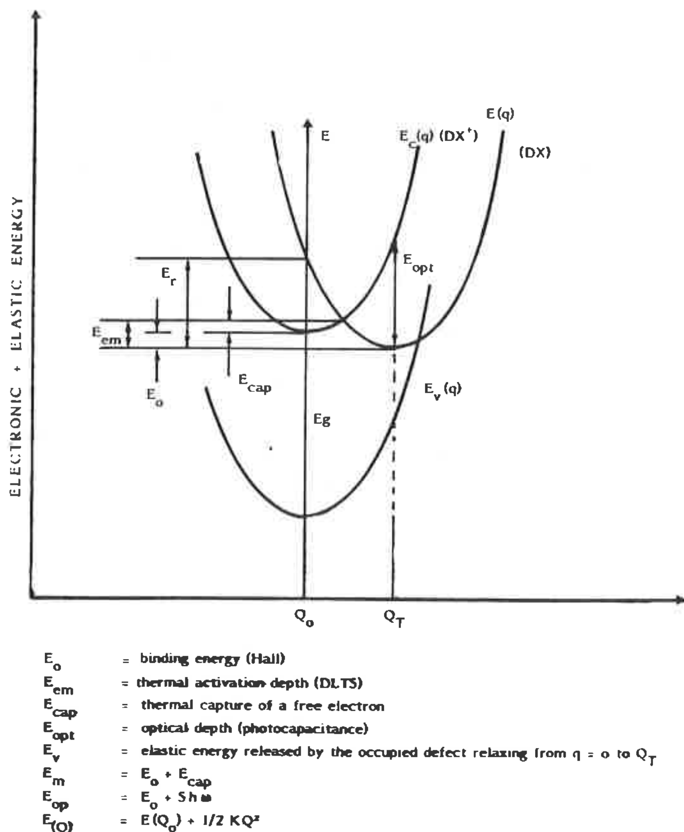

FIGURE 4. - *Configuration coordinate showing large lattice relaxation.*

details of the local structural, electronic, magnetic and lattice vibrational properties at the resonant atomic site [14-16]. Much of this information is unique to the Mössbauer effect, but some results can be compared directly to those of other techniques such as nuclear magnetic resonance and nuclear quadrupole resonance. The physics behind the observation of the Mössbauer effect and spectroscopic parameters that are relevant to the study of DX centers will be reviewed in the next section, followed by a discussion of the few experiments that have used Mössbauer spectroscopy to study DX centers. The last section will suggest possibilities of further experiments.

II. Mössbauer Spectroscopy

A basic requirement for observation of the Mössbauer effect is the presence of adequate concentrations of the appropriate isotope in both a solid-state source (isotope in nuclear excited state) and a solid-absorber (isotope in nuclear ground state). The "appropriate" isotope is limited to those that have a transition energy that is sufficiently low ($\leq$ 100 keV) that the probabilities for recoilless emission and absorption of the γ-ray yield an experimentally useful degree of resonance. The lifetime of the excited state is also important since this controls the resolution of the hyperfine interactions. Of the dopants currently known to exhibit DX behavior, only Sn and Te have isotopes that yield the Mössbauer effect : ^{119}Sn and ^{125}Te. The natural isotopic abundance of ^{119}Sn is 8.58 % while that of ^{125}Te is 6.99 %. Experimentally, the resonance is observed by producing a known, repetitive, relative motion (typically at constant acceleration) between the source and absorber so that the frequency of the γ-ray is modulated by the Doppler effect. Spectra are usually displayed as relative transmission or emission versus Doppler velocity. Energy widths, shifts, or splittings obtained from Mössbauer Spectroscopy are typically reported in units of the corresponding Doppler velocity. Useful unit conversions, constants data and complete bibliographies dedicated to the Mössbauer literature are available [17-20]. For ^{119}Sn and ^{125}Te 1 mm/s of Doppler velocity corresponds to 7.96 x 10^{-8} eV and 1.18 x 10^{-7} eV, respectively.

There are basically two types of Mössbauer experiments that can be performed to study DX centers : (1) those which make use of ^{119}Sn or ^{125}Te in the semiconductor host as resonant absorbers and (2) those which utilize the excited states, $^{119}Sn^*$ (23.9 keV) or $^{125}Te^*$ (35.5 keV), in the semiconductor host as resonant emitters. The latter experiments must deal with preparation, handling and characterization of radioactive materials while the former require simply the mounting of a standard radioactive source in the spectrometer. Aside from these practical safety considerations, both types of experiments suffer from special problems. Consider the absorber experiments first. Doping densities typically selected for the study of DX centers in $Al_xGa_{1-x}As$ are below about 5×10^{18} cm^{-3} in order to avoid complications associated with solid solubility limits and compensation resulting from the formation of non-DX related defects that are very likely to occur at higher levels. With currently available source strengths for ^{119}Sn and ^{125}Te studies, absorber experiments are limited to doping levels of $\geq 10^{18}$ cm^{-3} for ^{119}Sn [21-23] and $\geq 10^{19}$ cm^{-3} for ^{125}Te [24-25]. Both types of studied were aided by the use of 85-96 % ^{119}Sn and ^{125}Te isotopic enrichments of the dopant materials. Thus, there is a restricted range of doping, near the heavy end, where absorber Mössbauer measurements can be made. Multiple site occupation by Sn or Te must be considered in the search for the DX centers in such heavily doped specimens. In spite of this limitation, DX centers have recently been detected in ^{119}Sn-doped $Al_xGa_{1-x}As$ [23-26] and in ^{119}Sn-doped GaAs under pressure [27].

For the source experiments, an obvious advantage is that, in principle, much lower doping levels could be utilized ($\geq 10^{13}$ $^{119}Sn^*$ or $^{125}Te^*$ atoms/cm^3). However, radioactive parents of $^{119}Sn^*$ or $^{125}Te^*$ may be of low specific activity such that low doping levels would be difficult to achieve by doping during growth using conventional methods (LPE, MOVPE, MBE). We are not aware of any experiments that have attempted the study

of DX centers by doping radioactive parent isotopes during single crystal growth of $Al_xGa_{1-x}As$. An alternative method of doping/source preparation is via ion implantation of appropriate radioactive parent isotopes that decay into $^{119}Sn^*$ or $^{125}Te^*$. This method has been explored extensively for the case of $^{119}Sn^*$ to study a variety of parent isotopes in a wide variety of host semiconductors [28-30]. In many cases it also suffers from the problem of low specific activity so that effective concentrations in the thin implanted layer are about 0.1 % to 1 % (10^{19} to 10^{20} cm^{-3}). For the study of DX centers it is imperative that the radioactive parent isotope occupy the lattice site that is appropriate to enable the excited daughter Mössbauer isotope to become DX center, i.e. a group III site for $^{119}Sn^*$ and a group V site for $^{125}Te^*$. Of the possible $^{119}Sn^*$ parents (^{119}Cd, ^{119}In, ^{119m}Sn, ^{119}Sb, ^{119m}Te and ^{119}Xe), ^{119}In, ^{119}Cd and ^{119m}Sn preferentially occupy the group III site [28-31] while of the possible $^{125}Te^*$ parents (^{125}Sn, ^{125}Sb, ^{125m}Te, ^{125}I, ^{125}Te, ^{125}Xe, ^{125}Cs and ^{125}Ba), ^{125}Sb, ^{125m}Te, and ^{125}I are likely to preferentially occupy the group V site. After (or during) implantation, the radiation damage must be removed by annealing to electrically activate the implanted dopant, a process that may activate only a small fraction of the implanted atoms depending on the effective concentration of the implanted layer [32]. Source experiments must also consider possible complicating nuclear decay effects such as nuclear recoil alteration of lattice positions and electronic charge alteration [30]. We are aware of only three implantation/source experiments that have obtained Mössbauer data that may be related to DX centers [33-35] and these will be discussed below. The spectroscopic parameters obtained from the Mössbauer effect will now be reviewed.

II.1. Resonance Linewidth

The minimum experimental Mössbauer resonance linewidth, Γ_m (full-width at half-maximum resonance), is given simply by $2\ h/\tau$, where τ is the lifetime of the nuclear excited state that produces the recoilless γ-ray. For $^{119}Sn^*$ and $^{125}Te^*$ τ is 25.61 ns and 2.137 ns, yielding Γ_m = 0.65 mm/s and 5.2 mm/s, respectively. *Figure 5a* shows typical single-line spectra for ^{119}Sn and ^{125}Te Mössbauer effects. The observed linewidths, Γ_o, for ^{119}Sn are typically $\geqslant$ 0.8 mm/s due to self-absorption in the source and/or thickness broadening caused by the absorber [25, 36]. The minimum width for ^{125}Te has been observed for ^{125}Te-doped GaAs and the single line resonance was attributed to the shallow ionized donor site, Te_{As}^+ [24]. The value of Γ_o controls the experimental resolution, i.e. the ability to detect multiple sites of the dopant atoms through the hyperfine interactions (isomer, quadrupole, magnetic) which cause shifts and splitting of the resonance lines. The size of the shifts or splittings relative to Γ_o governs the accuracy and reliability of any interpretation.

II.2. Isomer Shift

Electrostatic interaction of electrons and nucleons produces a shift, the isomer shift [37], of the Mössbauer resonance energy that is proportional to the difference in electron density at the Mössbauer nucleus in the source, $\varrho_S(0)$, and in the absorber, $\varrho a(0)$:

$$\delta = \alpha\ [\varrho_a(0) - \varrho_S(0)] \quad (4)$$

Figure 5a illustrates δ for both ^{119}Sn and ^{125}Te Mössbauer effects. The measurement of δ is one of the very few methods which provides direct information on electronic wavefunctions. The proportionality constant α, depends on nuclear parameters that cannot be predicted and thus must be established by experimental determination of δ and theoretical values of $\varrho(0)$ for simple or well understood solids. Values of α for ^{119}Sn and ^{125}Te are approximately $+0.07\ a_o^3$ mm/sec [38, 39] and $+0.03\ a_o^3$ mm/s [40], respectively. Since experimental isomer shifts can be measured to a precision of about 0.01 Γ_o or better, then changes in $\varrho(0)$ larger than about 0.01 Γ_o/α can be detected. For ^{119}Sn this corresponds to $\Delta\varrho(0) \approx 0.1\ a_o^3$ and for ^{125}Te, $\Delta\varrho(0) \approx 2a_o^3$. Clearly the ^{119}Sn Mössbauer effect is more sensitive to changes in electron contact density than that of ^{125}Te.

Isomer shifts due to significant changes in valence electronic structure can be seen from *figure 5a* for ^{119}Sn [Sn^{2+} (ionic) in $CaSnO_3$ to Sn^{IV} (covalent) in $ZnSnAs_2$] and for ^{125}Te [Te (metallic) in Cu to $Te^{IV/2-}$ (covalent/ionic) in ZnTe]. The corresponding values of δ in these two cases (1.78 mm/s and -0.16 mm/s, respectively) yield changes in $\varrho(0)$ of $+25a_o^3$ and $-5a_o^3$, respectively, based on the above calibration constants. Much smaller changes in electronic structure are detectable. In fact, a change in 5s-like electronic character of only 0.01 of an electron could be detected for ^{119}Sn. However, the binding of a conduction band electron at a shallow donor site (Sn_{Ga} or Te_{As}) at very low temperature produces a $\Delta\varrho(0)$ that is too small to be observed due to the large spacial extent of this weakly bound electron. A deep donor electronic state such as the DX center should be much more localized and therefore a change in $\varrho(0)$ should be detectable between the ionized and ground states. Although several specific atomic scale models of the DX center have been proposed [41-47], to our knowledge there have not been any theoretical predictions of $\Delta\varrho(0)$ on the basis of such models.

II.3. Quadrupole Splitting

A Mössbauer isotope that is placed in an environment that has a point group symmetry less than cubic will experience the electric quadrupole interaction. For both ^{119}Sn and ^{125}Te, which have excited and ground-state nuclear spins of 3/2 and 1/2, respectively, this interaction results in a two line resonance with splitting [14-16].

$$\Delta = eQV_{zz}(1 + \eta^2/3)^{1/2}/2 \quad (5)$$

where Q is the nuclear quadrupole moment, $\eta = (V_{xx} - V_{yy})/V_{zz}$, V_{ii} are the components of the diagonalized electric field gradient (EFG) tensor evaluated at the nucleus and $|V_{zz}| \geqslant |V_{xx}| \geqslant |V_{yy}|$. For axial symmetry, e.g. tetragonal or trigonal symmetry, $V_{xx} = V_{yy}$ and $\eta = 0$. *Figure 5b* illustrates the quadrupole splitting for the specific case of Te metal (Δ = 7.45 mm/s).

The values of Q for ^{119}Sn and ^{125}Te are $-$ 0.064 barns and 0.20 barns, respectively [19], so that for equivalent EFG tensors the ^{125}Te Mössbauer effect yields about a 3-fold larger splitting. However, one should normalize this splitting by Γ_o as we did above for the isomer shift. Two lines of equal intensity are experimentally resolved, in the sense that the line shape is obviously flattened near maximum resonance, when $\Delta \approx \Gamma_o$. Thus the value of V_{zz} required for an experimentally obvious quadrupole splitting is $|V_{zz}| \geqslant 2\Gamma_o/eQ$, or approximately 0.7×10^{16} esu/cm^3 for ^{119}Sn and 2×10^{16} esu/cm^3 for ^{125}Te. Theoretical calculations [48] of V_{zz} for Te in Si or Ge with a nearest neighbor vacancy are consistent with experimental values of $V_{zz} \approx 1.2\times10^{16}$ esu/cm^3 and similar calculations for I in GaAs [49] suggest $V_{zz} \approx -0.7\times10^{16}$ esu/cm^3. We are not aware of theoretical calculations of Vzz for specific DX center models.

The transition probabilities for the two transitions ($\Delta m = \pm 3/2 \rightarrow \pm 1/2$ and $\pm 1/2 \rightarrow \pm 1/2$) yielding the quadrupole doublet (*figure 5b*) depend on the orientation of the principal axes of the EFG tensor relative to the γ-ray direction [14-16]. Thus, for a sample which has a unique or preferred orientation for the axes, the relative intensities of the doublet will, in general, not be unity. For example, and axially symmetric EFG tensor ($\eta = 0$) with symmetry axis at an angle 0 relative to the γ-ray direction produces a relative line intensity of :

$$\frac{I\ (\pm\ 3/2 \rightarrow \pm\ 1/2)}{I\ (\pm\ 1/2 \rightarrow \pm\ 1/2)} = \frac{1 + \cos^2\theta}{2/3 + \sin^2\theta} \quad (7)$$

This ratio can vary from 3 for the axis parallel to the γ-ray direction to 3/5 for the axis perpendicular to the γ-ray. A randomly oriented powder absorber yields a ratio of unity as is shown in *figure 5b* for Te metal powder. Specific models of DX centers that predict a unique or preferred orientation of the EFG tensor

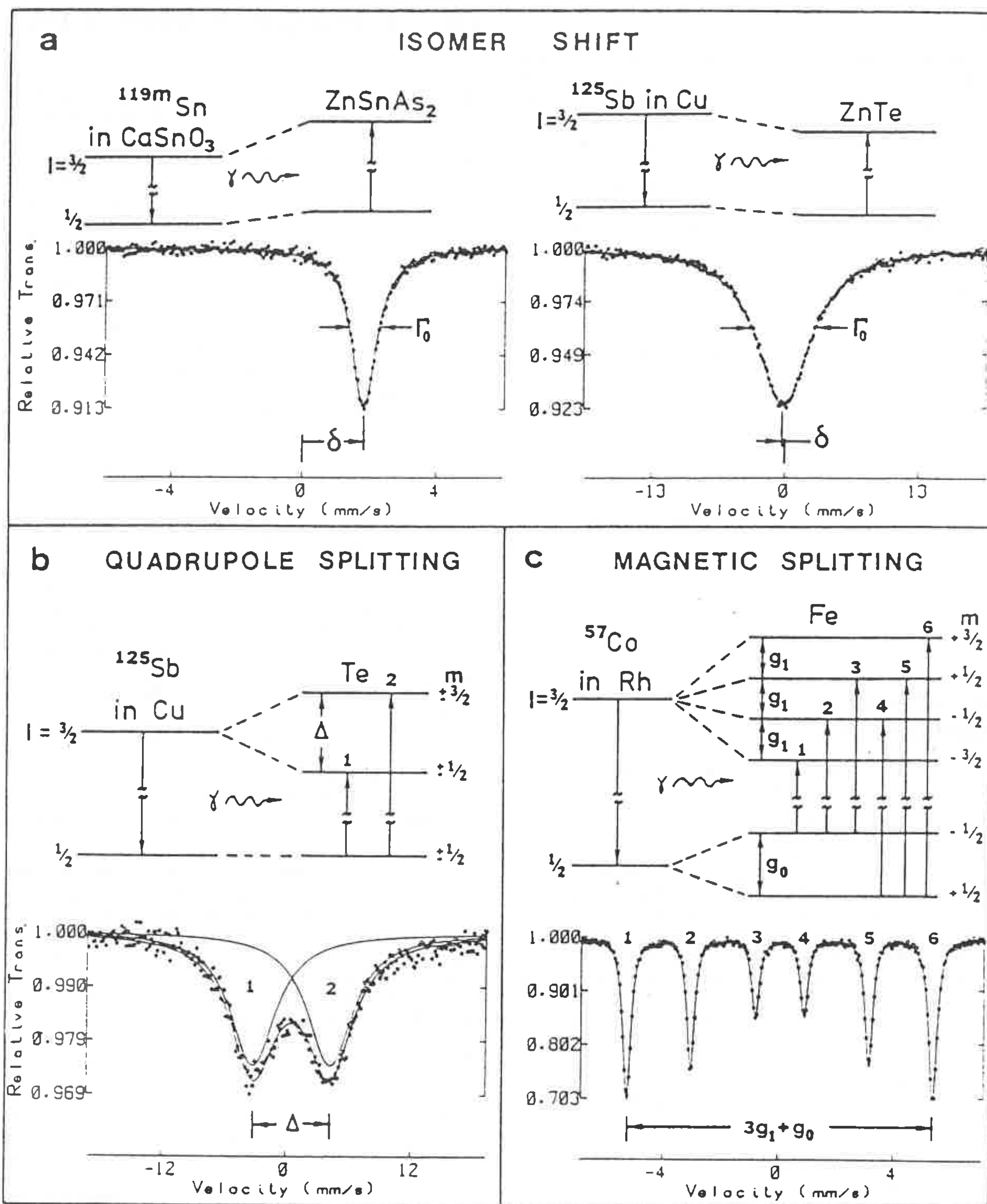

FIGURE 5. - *Hyperfine Interactions studied by Mössbauer Spectroscopy. Energy level diagrams illustrate the transitions, shifts, and splittings. Actual Mössbauer spectra are shown for various source-absorber combinations. Note the different velocity scales used for ^{119}Sn and ^{125}Te. The solid lines through the data points are least-square fits of Lorentzian-shaped resonance lines. Superpositions of Lorentzians are used in **b** (2, individually shown) and **c** (6). The magnetic hyperfine field in metallic Fe in **c** is given by $H = (3g_1 + g_0)31.06 = 33.0$ tesla at room temperature and is typically used for velocity calibration of spectrometers.*

at the ^{119}Sn or ^{125}Te site could be tested via angle-dependent studies of the relative line intensity. However, a site with trigonal symmetry along the <111> axes in GaAs, for example, would yield equal line intensities for any orientation of the single crystal sample with respect to the γ-ray direction due to averaging over all the <111> equivalent axes [50].

II.4. Magnetic Splitting

The presence of a magnetic field, H, at the nucleus of the Mössbauer isotope will produce a Zeeman splitting of the nuclear levels through the magnetic dipole interaction [14-16], as shown in *figure 5c*. The size of the splitting is directly proportional to H, which may originate from a net electronic spin density at the nucleus (due to an atomic magnetic moment) or from an exter-

nally applied field. For ^{119}Sn or ^{125}Te a six line magnetic resonance is observed provided the quadrupole interaction strength is small compared to that of the magnetic interaction. Two additional resonance lines may appear if the two interactions are comparable in strength [51]. No permanent dipole moment is expected for ^{119}Sn or ^{125}Te in a semiconductor host such as $Al_xGa_{1-x}As$, so a magnetic splitting will be observed only under an applied field. This approach may be useful in order to verify the existence of a quadrupole interaction as opposed to multiple isomer shifts due to multiple sites [52] and to obtain information on the orientation of the principal axes of the EFG tensor [15, 51]. For example, in the case of an axially symmetric EFG tensor with symmetry axis at angle β relative to the applied field direction, the quadrupole splitting is [14, 15] :

$$\Delta = eQV_{zz}(3\cos^2\beta - 1)/4 \quad (8)$$

This expression is valid for a quadrupole splitting that is small compared to the magnetic splitting. Experimentally, this may require field strengths of several tesla. For a single crystal sample one must take into account possible equivalent symmetry orientations of the principal axis, such as all <111> or <100> axes. For the γ-ray direction along a <100> direction and the EFG symmetry axes along the <111> directions, then $\cos^2\beta = 1/3$ for all <111> directions and $\Delta = 0$, so that a symmetric magnetic pattern would result. The relative line intensities of the magnetic spectrum are controlled by the direction of H relative to the γ-ray direction [4, 5]. Typically H is applied parallel to the γ-ray direction so the $\Delta m = 0$ transitions are missing and a four-line magnetic pattern is produced.

II.5. Recoilless Fraction and Quantitative Analysis

The probability for recoil-free emission or absorption of the γ-ray is known as the recoilless fraction and is given by [4, 6]

$$f = \exp(-k^2 \langle x^2 \rangle) \quad (9)$$

where k is the magnitude of the wavevector of the resonant γ-ray and $\langle x^2 \rangle$ is the mean-square displacement of the resonant nucleus along the γ-ray direction. Vibrational anisotropy can be studied through its effect on the relative line intensities of a quadrupole doublet [15]. This effect must be carefully separated from that due to the orientation effect on transition probabilities noted above. Lattice vibrational properties are thus accessible through measurements of relative line intensities or of f which are obtained typically from the integrated intensities (areas) of the resonance signals. In the limit of "thin" source and absorber (negligible self-absorption) [15, 36], the resonance area due to a unique crystallographic site in the source (with $f = f_s$) and a unique crystallographic site in the absorber (with $f = f_a$) is given by [53]

$$A = Kf_sf_an \quad (10)$$

where n is the number of absorber Mössbauer nuclei (in that site) per cm^2 in the γ-ray beam and K is a constant that depends on the particular Mössbauer isotope and also on a background correction factor that must be evaluated in each experiment. For absorber experiments K has been found to accuracies of about 10 % and 20 % for ^{119}Sn [21] and ^{125}Te [24], respectively. This allows absolute determination of either f_a or n if the other is known. By simply varying the temperature of the source of absorber f_s or f_a can be found (provided n is constant during this process) via ratios of A at two or more temperatures by comparison with either the Debye model [14-16] or by a more sophisticated analysis [29]. Values of f and corresponding Debye temperatures have been tabulated for Sn sites in GaAs and several relevant Sn compounds [21, 22]. The value of f = 0.55 at 77 K has been obtained for ^{125}Te on the As site in GaAs, corresponding to a Debye temperature of 250 K [24]. Quantitative determination of the number densities of ^{119}Sn on the Ga site in several GaAs samples provided evidence that as-grown samples are not compensated for doping densities up to about 5×10^{18} Sn/cm^3 [21, 22].

III. Microscopic structure of DX

At an early stage in the investigation of DX centers, Lang *et al.* proposed [56] and expanded upon a LLR model to explain PPC [57]. They introduced a configuration-coordinate model for the DX center and argued that its microscopic origin could be a complex involving a donor and an arsenic vacancy, V_{As}. Subsequently, evidence for a reduction in local symmetry at the DX center was provided by measurements of the attenuation of ballistic phonons [58]. Trigonal and orthorhombic symmetries for Sn and Te, respectively, were reported in support of a Sn-vacancy nearest-neighbor complex (Sn_{Ga}-V_{As}) and a Te-vacancy next-nearest-neighbor complex (Te_{As}-V_{As}) [58]. However, the existence of sufficient concentrations of V_{As} in $Ga_{1-x}Al_xAs$ grown by metal-organic vapor-phase epitaxy (MOVPE) or molecular-beam epitaxy (MBE), which both operate with a large excess of As vapor, is rather unlikely. The Mössbauer resonance of such a complex, Sn_{Ga}-V_{As}, should be significantly different from Sn_{Ga}, the shallow donor.

Since DX centers are defects that are suggested to be strongly coupled to the lattice, a model based on local effects due to Al alloying has been introduced by Kobayashi *et al.* [43]. The stability of the sp^3 bonding between donor and host surrounding atoms is considered in the indirect-band gap alloy regime. They assume that in instability in the sp^3 bond occurs due to the anisotropic distribution of Al and Ga atoms as nearest neighbors to the As site or next-nearest neighbors to the Ga site. The suggested result is a bond reconstruction of the donor atom on the As site into an sp^2– or even sp-like configuration. Specific modeling was done for Te and Si doping [43]. However, the DX center was shown to appear in GaAs under hydrostatic pressure above 3 GPa. Such results demonstrate that the emergence of the DX center is related to a change in band structure from GaAs to (GaAl)As-like, comparable to what happens in $Al_xGa_{1-x}As$ as x increases. In other words, the deep donor in $Al_xGa_{1-x}As$ does not depend on the formation of any chemical complex involving Al atoms or vacancies. High-pressure investigations provide evidence of large lattice relaxation.

Oshiyama and Ohnishi [44] proposed a model in which the donor Si atoms on the Ga site are surrounded by a distorted As tetrahedron. The model is supported by calculations of the energy-level structure of clusters. The antibonding state of the donor shifts downward in the band gap upon distortion of the As surroundings. It was suggested that this model could be extended to GaAs under pressure since the local presence of Al is not required to generate the deep level.

Morgan [45] pointed out that electrons bound to the donors can occupy either shallow or deep states. Transition between the two states involves a large lattice relaxation. The DX center deep state is derived from a triplet of symmetry T_2, the donor being displaced from its centered lattice position. This displacement resembles a Jahn-Teller effect, the origin of which was suggested as follows [45] : the T_2 state is formed from the four nearest-neighbor antibonding orbitals ; the component of this state having a symmetry axis along one of the <111> has 3/4 of the electron probability density in this orbital and only 1/4 in the other three ; displacing the central atom along <111> away from the nearest neighbor in this direction lowers the total energy of the state. Many of the experimental observations on DX centers are qualitatively explained by this model [45]. Hasegawa and Ohno [46] have also suggested that DX centers are antibonding states aristing from the donor impurities and that the shallow-deep-donor transition may require some lattice distortion to stabilize the antibonding state.

A recent new proposal is that the ground state of the DX centers is a negatively charged two electron state D^-. This occurs when U, the Hubbard correlation energy is negative. For $U < 0$, the electron-phonon interaction stabilizes two electrons state more strongly than a single electron one. Thus this model requires a large lattice relaxation. The ground state being D^-, the photo-ionization of DX centers involves two electrons bound to this

state according to

$$2d^0 \rightarrow d^+ + D^- \tag{11}$$

Theoretical evaluation by Chadi and Chang [47] indicates that a distortion is stabilized for D^-, this distortion consists of an off-center displacement of the group IV donor.

In contrast to all the models just discussed which imply large lattice relaxation other authors [59-62] have discussed the existence of DX centers as an effective mass state (EMS), involving little or no lattice relaxation. This EMS is associated with higher conduction bands [62] and its binding energy is increased due to central cell correlation arising from intervalley mixing [63].

IV. Discussion

IV.1. Shallow Donor Sites

The Mössbauer resonance of the shallow, substitutional donor site, Sn_{Ga}, has been identified in GaAs from both source [28, 29, 54] and absorber [21, 22] experiments. The isomer shifts and effective Debye temperatures agree very well as shown in *Table I*. The sources were prepared by ion-implantation doping of radioactive species [28, 54] and the absorbers were prepared by doping of enriched ^{119}Sn during growth of single-crystal layers by liquid-phase epitaxy (LPE) [21] and by metal-organic vapor-phase epitaxy (MOVPE) [22]. The absorber experiments demonstrated a one-to-one correspondence between the free electron density (via Hall measurements) and the number density of Sn_{Ga} sites (via quantitative Mössbauer analysis) for densities up to about 5×10^{18} cm^{-3}. This lack of compensation is consistent with the absence of the Sn_{As} acceptor site or other shallow acceptor sites [21, 22] in as-grown Sn-doped GaAs.

The shallow Sn donor site in a series of $Al_xGa_{1-x}As$ alloys yields isomer shifts that are not distinguishable from that in GaAs [23]. This is consistent with the fact that the nearest neighbor environment of the Sn does not change with x and that the Mössbauer resonance is relatively insensitive to second neighbor shell alterations in tetrahedrally coordinated systems [55]. The value of the isomer shift of Sn_{Al} in AlAs is included in *Table I*. Hall measurements were not made on the Sn-doped AlAs since a protective coating of GaAs was requiered to prevent oxidation [23]. Thus a correlation between the SnAl site density and the free electron density in AlAs has not yet been made.

IV.2. DX centers

The Mössbauer resonance of ^{119}Sn-doped $Al_xGa_{1-x}As$ layers grow by MOVPE was observed to be dramatically altered for x = 0.3 to 0.43 compared at x = 0 or x = 1 [23]. These data are shown in *figure 6*. Since the DX center site population is well known to maximize at compositions of x = 0.3 to 0.4 similar to the results shown in *figure 7*, the altered resonance was interpreted in terms of Sn DX center formation in this composition range. Three Lorentzian lines were fitted to all spectra versus x and the systematic increase of two of the lines (lines 2 and 3 in *figure 6*) at the expense of the one due to Sn on the group III site (line 1 in *figure 6*) led to a straightforward interpretation : the two line fit is due to a quadrupole splitting at a Sn DX site that has non-cubic symmetry. The spectral parameters from this interpretation are shown in *Table II*. The size of the isomer shift is consistent with significant electron localization [23, 26] and the size of the splitting is consistent with a large lattice relaxation away from cubic symmetry. However, the unresolved nature of the two-line fit to the data permits alternate interpretations such as the possibilities of two types of Sn DX centers or even a distribution of centers, both of which have been reported in the literature [64, 66]. In such cases one does not require a quadrupole splitting to explain the data. Thus, a definite conclusion on the issue of a

TABLE I. - *Mössbauer determined parameters of shallow Sn donors in $Al_xGa_{1-x}As$. δ is the isomer shift of the donor site at 77 K relative to a standard material at room temperature ($CaSnO_3$ for ^{119}Sn). θ is the Debye temperature and f the corresponding recoilles fraction at 77 K. Experimental uncertainties are given in parentheses.*

Donor site	Host (x)	δ (mm/s)	θ (K)	f	Doping Method	Ref.
Sn_{Ga}	0	1.83 (3)	202 (5)	0.67	Implantation	29
Sn_{Ga}	0	1.83 (3)	175 (20)	0.60	LPE growth	21
Sn_{Ga}	0	1.80 (2)	200 (10)	0.66	MOVPE growth	22
Sn_{III}	0.20	1.78 (2)			MOVPE growth	23
Sn_{III}	0.76	1.81 (4)			MOVPE growth	23
Sn_{Al}	1	1.75 (4)			MOVPE growth	23

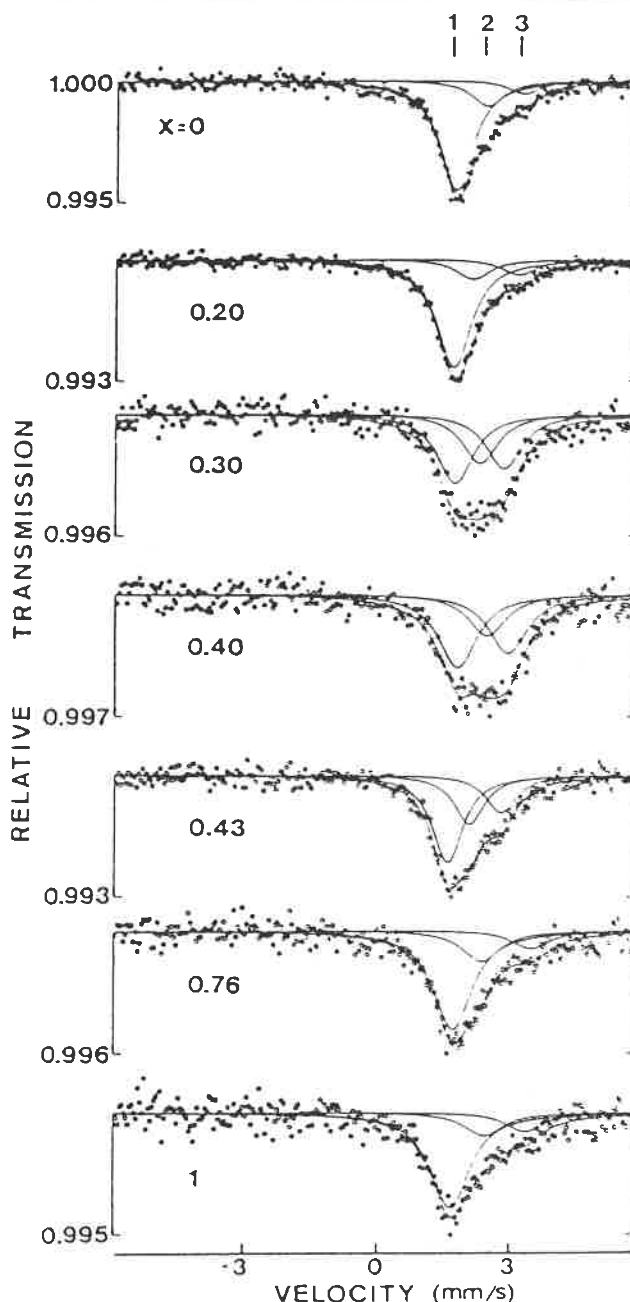

FIGURE 6. - *^{119}Sn Mössbauer spectra from a series of ^{119}Sn-doped $Al_xGa_{1-x}As$ alloys prepared by MOVPE. Each spectrum is fitted with a superposition of 3 Lorentzian lines as indicated (from ref. 23).*

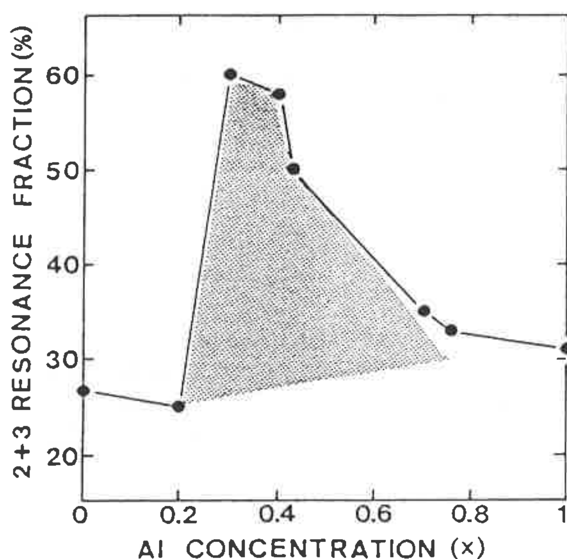

FIGURE 7. - *Summed Mössbauer resonance fraction of lines 2 and 3* (figure 6) vs *Al concentration. Shaded region is attributed to Sn DX centers (from ref. 23).*

TABLE II. - *Mössbauer spectral parameters of Sn DX centers. δ is the isomer shift of the DX center at 77 K relative to a standar at room temperature ($CaSnO_3$ for ^{119}Sn). Δ is the quadrupole splitting at 77 K. A bracket around the value indicates that this parameter is not yet established due to alternate interpretations.*

DX Site	Host	δ (mm/s)	Δ (mm/s)	Doping Method	Ref.
Sn	$Al_xGa_{1-x}As$ (x = 0.3-0.43)	2.67 (5)	[0.6 (1)] or [0]	MOVPE growth	23
Sn	GaAs at 3.3 to 4.8 GPa	2.60 (5)	[0.4 (1)] or [0]	MOVPE growth	27

large lattice relaxation at DX centers cannot be made on the basis of this study [23].

A new interpretation of the ^{119}Sn-doped $Al_xGa_{1-x}As$ Mössbauer data (shown in *figure 6* [23]) has recently been proposed to support a specific microscopic model based on an antisite defect that requires the localization of three electrons [67]. A key feature of the Mössbauer results that were used for this interpretation is that the resonance due to the shallow Sn_{Ga} site remains at a significant fraction (35-40 %) of the total in the range of x where maximum DX formation occurs. The DX fraction is indicated by the shaded area of *figure 7*. This provides evidence that the Sn DX center is a multi-electron trap since localization of a single electron would cause the disappearance of the Sn_{Ga} resonance. One problem with the interpretation [67] is that the DX center resonance was attributed to only one of the two fitted lines (line 3 on *figure 7*). This appears inconsistent with the proposed atomic-scale nature of the defect [42, 67] which should produce a quadrupole split signal.

High pressure Mössbauer experiments have very recently been reported [27] that confirm the previous identification Sn DX centers [23], and provide strong support for localization of two or more electrons in the Sn DX ground state. A ^{119}Sn-doped GaAs layer grown by MOVPE, previously characterized by Hall measurements to have a free carrier density of $6x10^{18}$ cm^{-3} and by Mössbauer measurements to have a total Sn concentration of $8x10^{18}$ cm^{-3} [22], was subjected to pressures of up to 4.8 GPa. As shown in *figure 8*, new resonance appeared with an isomer shift of 2.6 mm/s, in close agreement with the value associated with the Sn DX center in $Al_xGa_{1-x}As$ [23] *(Table II)*. This rules out the possibility that only line 3 in *figure 6* is due to Sn DX centers [67]. Also, the Sn_{Ga} resonance fraction remained near 50 % even at the highest pressure where essentially 100 % localization of the conduction electrons is expected. Detailed spectral analysis was made on the basis of two types of fits to the data and the results were interpreted under two assumptions [27] : one which attributed a quadrupole-split resonance to the DX center (as indicated in *figure 8*), even at zero pressure and one which attributed a single-line resonance to the DX center formed only at high pressure. Both assumptions require each DX center to trap more than one electron in order to be consistent with the Hall data. However, as was the case for the $Al_xGa_{1-x}As$ study [23], the issue of a large symmetry-breaking lattice relaxation is not yet resolved since the pressure-induced resonance could be adequately fitted without requiring a quadrupole doublet.

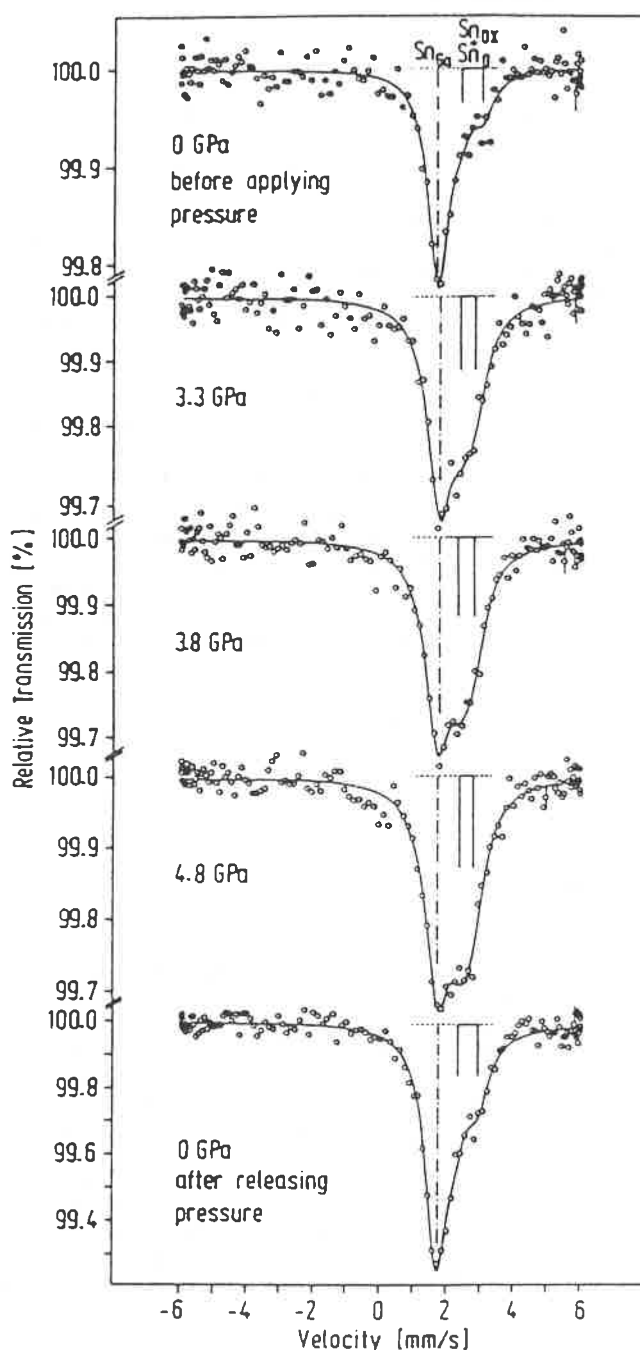

FIGURE 8. - *^{119}Sn Mössbauer spectra from ^{119}Sn-doped GaAs absorber under high pressure. The enhanced resonance near 2.6 mm/s produced by pressure is similar to the enhanced resonance caused by Al alloying shown in* figure 6 *and is attributed to Sn DX centers (from ref. 27).*

V. Isomer Shift

For ^{119}Sn, changes in $\varrho(0)$ are produced primarily by change in the 5s-like valence electron occupation number n_s, although substantial changes in 5p-like and 5d-like occupation number n_p and n_d change $\varrho(0)$ because of their shielding effect on 5s-electrons. In solids, the occupation numbers of valence electrons are non-integers and realistic numbers should be deduced from band structure calculations. Recently Svane [68] and Antoncik [69, 70] calculated $\varrho(0)$ in several compounds containing tin in an effort to establish the proportionality constant between δ and $\varrho(0)$. Their calibration will be used as a starting point for discussing the electronic structure of Sn in $Al_xGa_{1-x}As$. *Figure 9* shows the δ vs $\varrho(0)$ correlation for different tin compounds together with the calculated electronic configurations. Since a detailed theoretical investigation of the electronic structure of Sn in (GaAl)As is beyond the scope of the present paper, we use an approximation discussed by Antoncik.

$$\varrho(Sn)(n_s,n_p) = 61.0\ n_s - 8.25\ n_s^2 - 3.3\ n_s\ n_p \qquad (12)$$

which is found to give a reasonable agreement between δ and the theoretical fit of Svane and Antoncik [69] (squares on *figure 9*). Equation (12) will be used in the following discussion as an approximate means of estimating the Sn electronic structure.

V.1. *Electronic structure of SnGa and SnAl in $Al_xGa_{1-x}As$*

The electronic configurations of Ga and As in GaAs deduced from a tight binding approximation are $5s^{1.48}\ 5p^{1.38}$ and $5s^{1.54}\ 5p^{3.60}$ [71] respectively. When an atom acts as an electrically active impurity in a semiconductor the correct evaluation of its electronic configuration should involve compression effects. Furthermore, the electronic structure of the host semiconductor and its influence on the impurity are to be taken into account also. These features have been discussed by Gu [73] and his main conclusions can be summarized as follows : In the case of Sn_{Ga} in GaAs, it is of very little importance whether this level is occupied or not ; the wave function associated with a shallow donor is highly delocalized and does not contribute to $\varrho(0)$. The best agreement with δ corresponds to Sn donors having three valence electrons and transferring no charge to the neighbouring As atoms. Then, in this evaluation the occupancy numbers of Sn_{Ga} in GaAs are $5s^{1.28}\ 5p^{1.72}$ and the corresponding δ calculated according to Eqs. (4) and (12) is plotted in *figure 9*. The electronic structure of Sn_{As} in AlAs was estimated to be $5s^{1.21}\ 5p^{1.26}\ 5d^{0.12}$. Antoncik and Gu [70] discussed the limits of validity of their evaluation ; they argue that the lack of relevant information on the compression effect does not allow one to give a unique value for U(Sn) the extra potential produced in the Hamiltonian by the Sn impurity. A redistribution of the electrons of the Sn atom could also be restricted to $\delta\ n_s(Sn) + \delta\ n_p(Sn) = 0$: in this case the deduced occupation numbers for Sn_{Ga} would be $5s^{1.19}\ 5p^{1.67}$ which gives the same value for $\varrho(0)$ *(figure 9)*.

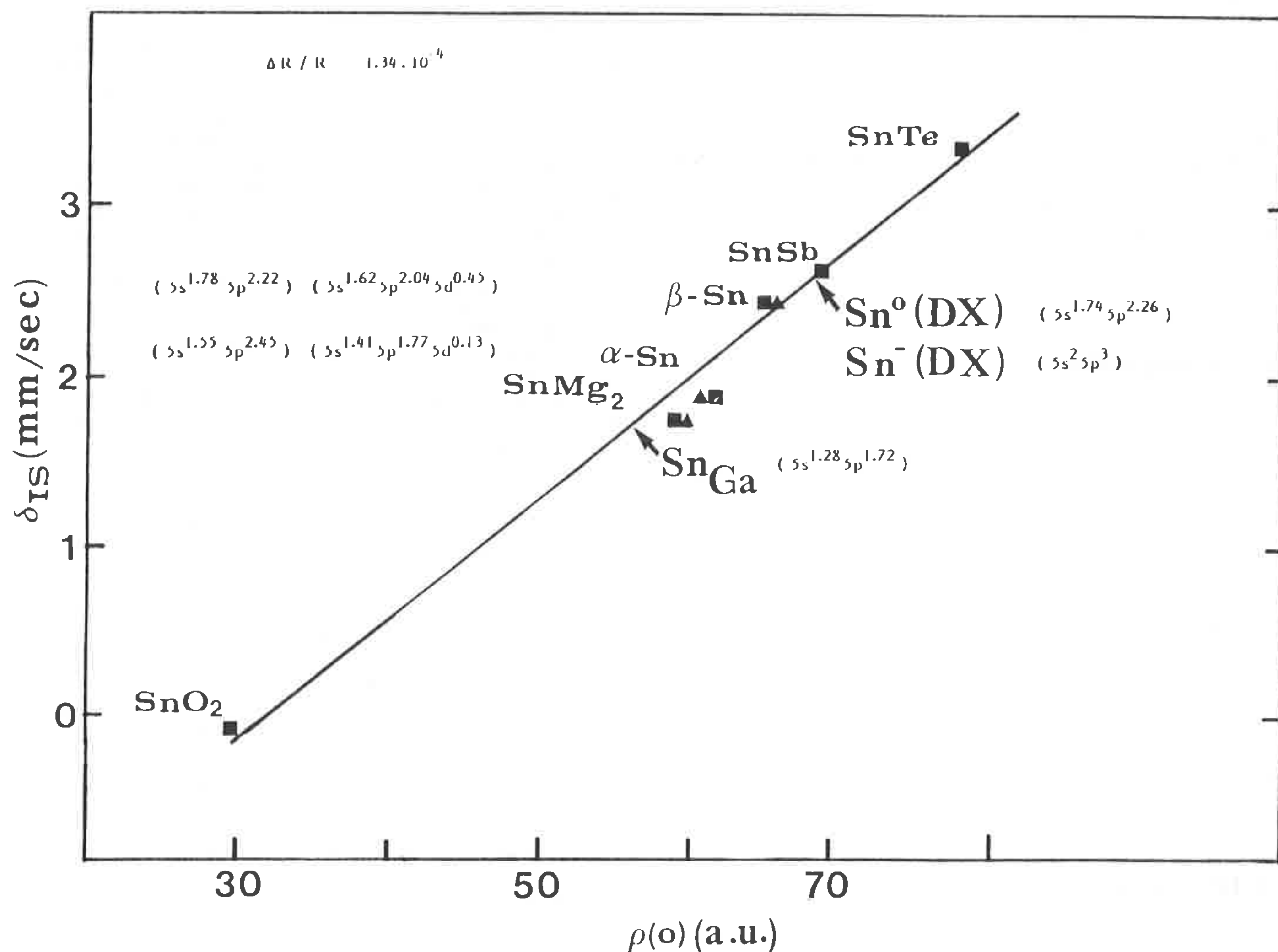

FIGURE 9. - *Measured IS in tin compounds* vs *the calculated electron densities - occupation numbers are given according to Svane [68] or calculated in a light binding approximation.*

V.2. Electronic Structure of Sn DX-center in $Ga_{1-x}Al_xAs$

The information brought by MS is that the DX centers attributed to lines 2 and 3 in *figure 5* for x = 0.3 – 0.4 could be either ; (i) a single substitutional atom with a quadrupole splitting ; (ii) two or more deep Sn-related centers in undistorted symmetry ; or (iii) even a distribution of similar centers. In all cases the electronic structure is quite different from that of the Sn_{Ga} shallow donors (SD). The occupancy numbers of 5s electrons in DX centers - deduced from Eqs. (4) and (12) and δ values of lines 2 and 3 - exceed by 0.4 to 0.6 electron those of the Sn_{Ga} (Sd). As suggested by various atomic-scale DX models, the hybridization of s and p orbital in DX centers is completely different from the SD, and even different from donors tied to the X valley (like Sn in AlAs). Thus photoionization of a DX center involves not only the transfer of an electron to the Γ valley, but also a bond reconstruction. If we assume a unique Sn– DX center, then lines 2 and 3 correspond to a quadrupole splitting. In this case, δ = 2.67 mm/s, Δ = 0.6 mm/s. According to Eqs. (4) and (12) the electronic structure would be $5s^{1.74}\,5p^{2.25}$, and the observed quadrupole splitting means that a significant local distortion of the As surrounding occurs. This is in agreement with DX models involving local distortion [44-47]. However, the information brought by the IS should be reconsidered as discussed in III on the assumption that the DX center traps more than one electron. It should be pointed out that the population of remaining Sn_{Ga} in either $Al_xGa_{1-x}As$, x > 0.3 or GaAs for p > 3 GPa is much higher than predicted from the classical behaviour of DX states, i.e., for x = 0.4 or p = 4 GPa, at low temperature all n-type impurities give DX centers, n_{SD} is almost zero. Thus, the remaining population of Sn_{Ga} should be Sn^{+}_{Ga} according to :

$$2\,Sn^{o} \rightarrow Sn_{Ga}^{+} + Sn_{DX}^{-} \qquad (13)$$

Whether the free electron coming from Sn is present or not, does not change the value of δ for SD(Sn_{Ga}). Assuming, for simplicity an unique DX center with Δ = 0.6 mm/s, the straighforward calculation of n_s and n_p from Eq. (12) gives for the DX center, i.e., Sn^{-}_{Ga} (with large lattice relaxation), $5s^2\,5p^3$.

VI. Conclusion

In conclusion, the value of Sn as DX state, whatever the model (positive or negative U center) means that hybridization of s and p orbital is completely different from the shallow donor. Furthermore, most likely, Δ is different from 0 and this means that a significant local distorsion of the As surrounding occurs. Under photoionization, one or possibly two electrons are transferred to the Γ valley, and a bond reconstruction around the Sn atom occurs. Thus, MS has proven to be a pertinent method for studying impurities in semiconductors, even to deduce electronic structure and also to assess their stability in the case of substitutional Sn in $Al_xGa_{1-x}As$ and in GaAs under hydrostatic pressure.

Acknowledgements : Discussions with Dr J. Moser regarding external magnetic fields are gratefully acknowledged.

References

[1] D.V. Lang, *in* Deep Centers in Semiconductors (S.T. Pantelides ed.), Gordon and Breach, New York, **1985**, p. 489 ; Physics of DX centers in GaAs Alloys (J.C. Bourgoin, ed.), *Sci-Tech. Publication*, **1990** ; P.M. Mooney, *J. Appl. Phys.*, **1990**, *67*, R1 ; K. Khacharuryan and K. Malloy, to be published, **1990** ; D.V. Lang, R.A. Logan, M. Jaros, *Phys. Rev. B*, **1979**, *19*, 1015.
[2] A.J. SpringThorpe, F.D. King, A Becke, *J. Electron Mater*, **1975**, *4*, 101.
[3] A.K. Saxena, *Phys. Status Solidi B*, **1979**, *96*, K77 ; *Appl. Phys. Lett.*, **1980**, *36*, 79 ; *J. Phys. C*, **1980**, *13*, 4323 ; *Phys. Status Solidi B*, **1981**, *105*, 777.
[4] H.J. Lee, L.Y. Juravel, J.C. Woolley, A.J. SpringThorpe, *Phys. Rev. B*, **1980**, *21*, 659.
[5] N. Lifshitz, A. Jayaraman, R.A. Logan, H.C. Card, *Phys. Rev. B*, **1980**, *21*, 670.
[6] N. Chand, T. Henderson, J. Klem, W. Ted Masselink, R. Fisher, Y.C. Chang, H. Morkoç, *Phys. Rev. B*, **1984**, *30*, 4481.
[7] E. Shubert, K. Ploog, *Phys. Rev. B*, **1984**, *30*, 7021 ; H. Künzel, K. Ploog, P.L. Zhou, *J. Electron. Mater*, **1984**, *13*, 281.
[8] T.N. Theis, *in* Proceedings of the 14th International Symposium on GaAs and Related Compounds, IOP Conf. Ser. Proc. n° 91, (A. Christou, H.S. Rupprecht, eds), IOP, Bristol, **1988**, p. 1.
[9] M. Watanabe, H. Maeda, *Jpn. J. Appl. Phys.*, **1984**, *23*, L734.
[10] M. Mizuta, K. Mori, *Phys. Rev. B*, **1988**, *37*, 1043.
[11] A.R. Regel, P.P. Seregin, *Sov. Phys. Semicond*, **1984**, *18*, 723.
[12] D. L. Williamson, *Hyp. Int.*, **1988**, *40*, 249.
[13] A. Nylandsted-Larsen, J.W. Pertersen, G. Weyer, *Mat. Sci. Forum*, **1989**, *38-41*, 1137.
[14] G.K. Wertheim, Mössbauer Effect : Principles and Applications, Academic press, New York, **1964**.
[15] V.I. Goldanskii, R. Herber eds, Chemical Applications of Mössbauer Spectroscopy, Academic Press, New York, **1968**.
[16] L. May, eds, An Introduction to Mössbauer Spectroscopy, Plenum Press, New York, **1971**.
[17] A.H. Muir Jr., K.J. Ando, H.M. Coogan, eds, Mössbauer Effect Data Index 1958-1966, Interscience, New-York, **1966**.
[18] J.G. Stevens, V.E. Stevens, P.T. Deason Jr., A.H. Muir Jr., H.M. Coogan, R.W. Grant, eds., Mössbauer Effect Data Index 1966-1968, IFI/Plenum, New York, **1975**.
[19] J.G. Stevens, V.E. Stevens, Mössbauer Effect Data Index 1969-1976, IFI/Plenum, New York, **1970-1978**.
[20] Mössbauer Effect Reference and Data Journal, Mössbauer Effect Data Center, University of North Carolina, Ashville, **1978** to present.
[21] D.L. Williamson, *J. Appl. Phys.*, **1986**, *60*, 3466.
[22] D.L. Williamson, P. Gibart, B. El Jani, K. N'Guessan, *J. Appl. Phys.*, **1987**, *62*, 1739.
[23] P. Gibart, D.L. Williamson, B. El Jani, P. Basmaji, *Phys. Rev. B*, **1988**, *38*, 1885.
[24] D.L. Williamson, P. Gibart, *J. Phys. C.*, **1981**, *14*, 2517.
[25] D.L. Williamson, M. Kowalchik, A. Rocher, P. Gibart, *Rev. Phys. Appl.*, **1983**, *18*, 475.
[26] P. Gibart, D.L. Williamson, B. El Jani, P. Basmaji, *in* Proceedings of the 14th Int. Symposium on GaAs and Related Compunds, IOP Conf. Ser. Proc. N° 91, (A. Christou, H.S. Rupprecht, eds), **1988**, 377.
[27] P. Gibart, D.L. Williamson, J. Moser, P. Basmaji, *Phys. Rev. Lett.*, **1991**, *65*, 1144.
[28] G. Meyer, J.W. Petersen, S. Damgaard, H.L. Nielsen, J. Heinemeier, *Phys. Rev. Lett.*, **1980**, *44*, 155.
[29] O.H. Nielsen, F.K. Larsen, S. Damgaard, J.W. Pertersen, G. Weyer, *Z. Phys. B*, **1983**, *52*, 99.
[30] J.W. Petersen, G. Weyer, H. Loft Nielsen, S. Damgaard, W.J. Choyke, H. Andreasen, *Hyp. Int.*, **1985**, *23*, 17.
[31] K. Bonde-Nielsen, H. Grann, H. Haas, F.T. Pedersen, G. Weyer, *in* 13th Int. Conf. on Defects in Semiconductors, (L.C. Kimerling and J.M. Parsey Jr., (eds), AIME, New York, **1985**, 1065.
[32] S.J. Pearton, J.S. Williams, K.T. Short, S.T. Johnson, D.C. Jacobsen, J.M. Poate, J.M. Gibson, D.O. Boerma, *J. Appl. Phys.*, **1989**, *65*, 1089.
[33] L. Niesen, D.O. Boerma, Z. Yi Qun, *Hyp. Int.*, **1987**, *35*, 729.
[34] G. Langouche, D. Schroyen, H. Bemelmans, M. Van Rossum, W. Deraedt, M. de Potter, *Mat. Res. Symp. Proc.*, **1988**, *104*, 527.

[35] G. Langouche, H. Bemelmans, J. Odeurs, G. Borghs, M. de Potter, W. Deraedt, M. Van Rossum, *in* Proc. 15th Int. Conf. on Defects in Semiconductors, Budapest, **1989**, in press.
[36] S. Margulies, J.R. Ehrman, *Nucl. Instrum. Meth.*, **1961**, *12*, 131.
[37] G.K. Shenoy, F.E. Wagner, eds., Mössbauer Isomer Shifts, North-Holland, Amsterdam, **1978**.
[38] A. Svane, E. Antoncik, *Phys. Rev. B*, **1986**, *34*, 1944.
[39] P.A. Magill, L.D. Roberts, *Phys. Rev. B*, **1988**, *37*, 399.
[40] S.L. Ruby, G.K. Shenoy, *in* ref. [37], p. 617.
[41] D.V. Lang, R.A. Logan, M. Jaros, *Phys. Rev. B*, **1979**, *19*, 1015.
[42] J.A. Van Vechten, *Mat. Res. Soc. Symp. Proc.*, **1985**, *46*, 83.
[43] K. Kobayashi, Y. Uchida, H. Nakashima, *Jpn. J. Appl. Phys.*, **1985**, *24*, L928.
[44] A. Oshiyama, S. Ohnishi, *Phys. Rev. B*, **1986**, *33*, 4320.
[45] T.N. Morgan, *Phys. Rev. B*, **1986**, *34*, 2664.
[46] H. Hasegawa, H. Ohno, *Jpn. J. Appl. Phys.*, **1986**, *25*, L319.
[47] D.J. Chadi, K.J. Chang, *Phys. Rev. lett.*, **1988**, *61*, 873 ; *Phys. Rev. B.*, **1989**, *39*, 10063.
[48] M. Van Rossum, I. Dezsi, K.C. Mishra, T.P. Das, A. Coker, *Phys. Rev B*, **1983**, *28*, 6086.
[49] M. Van Rossum, G. Langouche, K.C. Mishra, T.P. Das, *Phys. Rev. B*, **1983**, *28*, 6086.
[50] T.C. Gibb, *J.C.S. Dalton Trans.*, **1978**, 743 ; T.W. Guettinger, D.L. Williamson, *Phys. Rev. B*, **1979**, *20*, 3938.
[51] W. Kündig, *Nucl. Instrum. Meth.*, **1967**, *48*, 219.
[52] E.AA. Görlich, K. Latka, J. Moser, *Hyp. Int.*, **1989**, *49*, 723.
[53] A.H. Muir Jr. *in* Mössbauer Effect Methodology, Vol. 4, (I.J. Gruverman, Ed.), Plenum, New York, **1968**, p. 75.
[54] G. Weyer, S. Damgaard, J.W. Petersen, J. Heinemeier, *J. Phys. C.*, **1980**, *13*, L181.
[55] M.A. Ryan, M.W. Peterson, D.L. Williamson, J.S. Frey, G.E. Maciel, B.A. Parkinson, *J. Mater Res.*, **1987**, *2*, 528.
[56] D.V. Lang, R.A. Logan, *Phys. Rev. Lett.*, **1977**, *39*, 635.
[57] R.J. Nelson, *Appl. Phys. Lett.*, **1977**, *31*, 351.
[58] V. Narayaramurti, R.A. Logan, M.A. Chin, *Phys. Rev. Lett.*, **1979**, *43*, 1536.
[59] J.C.M. Henning, J.P.M. Ansems, *Semicond. Sci. Technol.*, **1987**, *2*, 1.
[60] E. Yamaguchi, *Jpn. J. Appl. Phys.*, **1986**, *25*, L643.
[61] H.P. Hjalmarson, T.J. Drumond, *Appl. Phys. Lett.*, **1986**, *48*, 656.
[62] J. Bourgoin, A. Mauger, *Appl. Phys. Lett.*, **1988**, *53*, 749.
[63] F. Bassani, G. Ladonisi, B. Preziosi, *Rept. Prog. Phys.*, **1974**, *37*, 1099.
[64] B. Balland, R. Blondeau, L. Mayet, B. Decremoux, P. Hirtz, *Thin Solid Films*, **1980**, *65*, 275.
[65] P.M. Mooney, N.S. Goswell, P.M. Soloman, S.L. Wright, *Mater Res. Symp. Proc.*, **1985**, *46*, 403.
[66] P.M. Money, T.N. Theis, S.L. Wright, *Appl. Phys. Lett.*, **1988**, *53*, 2546.
[67] J.A. Van Vechten, *J. Phys., Condensed Matter*, **1989**, *1*, 5171.
[68] A. Svane, E. Antoncik, *Phys. Rev. B*, **1986**, *34*, 1944 ; *Phys. Rev. B*, **1987**, *35*, 4611.
[69] E. Antoncik, *Phys. Sat. Sol. B*, **1977**, *179*, 605.
[70] E. Antoncik, B.L. Gu, *Physica Scripta*, **1982**, *25*, 836.
[71] B.L. Gu, *Thesis*, Aarhus University, **1982**.